Cu HyBrID Laser Kinetics: Optimization of HBr Partial Pressure and Buffer-Gas Flow Rate

Richard P. Mildren

***Abstract*—A detailed investigation into the dependence of the densities of the principal plasma species in the laser discharge on the buffer-gas operating parameters is reported. Simple expressions for the densities of the Cu, Br, and H species are derived by considering their major mechanisms for production and loss. These predict that the atomic Cu and Br densities are proportional to the HBr mass flow rate, whereas the density of H species (i.e., H and H_2) is proportional to the added HBr partial pressure. The theory agrees well with "Hook" method measurements of Cu density in a 25-mm bore diameter device; the Cu density increases approximately in proportion to the HBr mass flow rate, whereas it depends only weakly on the HBr partial pressure. Measurements of the fraction of Cu atoms excited by the discharge pulse, the rate of regrowth of the ground-state Cu density during the inter-pulse period, and the pre-pulse plasma impedance, are also explained in accordance with the theory. The results show that the plasma conditions for maximum laser output, which are remarkably similar to those of other "halogen enhanced" Cu lasers, can be achieved more directly by adjusting the overall buffer flow rate with the partial pressure of the added HBr fixed at 1–2 mbar. The theory is also useful for predicting optimum buffer-gas conditions for a wide range of Cu HyBrID laser dimensions and operating conditions.**

***Index Terms*—Bromine compounds, copper materials/devices, density measurement, gas lasers, hydrogen, spectroscopy.**

I. Introduction

In Cu "HyBrID" lasers, the HBr gas added to the Ne buffer-gas reacts with the discharge and Cu pieces placed in the tube bore to generate free Cu lasant atoms in a process that is intrinsically decoupled from the tube temperature in the range 450 °C–850 °C [1]. This method has the important advantage that the rate of Cu production is not sensitive to the balance of input power and thermal insulation, providing stable and efficient operation over a wide range of input powers without needing to carefully control the tube temperature. The HBr additive also has a secondary but very significant effect on the discharge kinetics. Like the other "halogen enhanced" Cu lasers utilizing hydrogen and halogen species in the discharge, i.e., the kinetically enhanced copper vapor laser (H_2:HCl:Ne-Cu vapor laser [2]) and the CuBr laser with H_2 additive (H_2:Ne:CuBr laser [3], [4]), much higher output powers and efficiencies ($>$ twofold) are obtained compared to conventional Cu lasers. Indeed, as far as the author is aware, the highest specific output power [5], efficiency [6], and high-beam quality output [7] of all Cu vapor lasers have been obtained from the HyBrID class.

Manuscript received July 16, 2002; revised October 28, 2002. This work was supported by the Australian Research Council Large Grant and Postdoctoral Fellowship awards.

The author is with the Centre for Lasers and Applications, Macquarie University, NSW 2109, Australia.

Digital Object Identifier 10.1109/JQE.2003.809325

Due to this dual role of the HBr in the discharge, optimization of the buffer-gas conditions is not as straightforward as for the non-HyBrID "halogen-enhanced" lasers. Numerous studies into Cu HyBrID laser performance as functions of the buffer-gas parameters [5]–[10] show that maximum output occurs when HBr is added to the discharge tube using a continuous flow of a Ne-HBr gas mixture with the HBr partial pressure typically 2%–10% (1–5 mbar) of the total tube pressure (10–100 mbar). The optimum buffer-gas flow rates correspond to the displacement of the tube volume every 10–60 s for small bore devices ($<$ 25 mm diameter) [11], [12] and every few minutes for the larger devices (40-80 mm diameter) [5], [8]. Recently, it was discovered that the continuous addition of the buffer-gas mixture is necessary to counter for the loss of the Br reactant which diffuses from the discharge zone [13]. However, the partial pressures of the lasant vapor and the species that enhance performance are dependent on plasma reactions and processes that are not well understood. As a result, only empirical methods have been used to date to optimize buffer-gas parameters.

In order to predict optimal buffer-gas conditions when varying tube design or operating parameters, it is important to have a more detailed knowledge of their effects on plasma composition and kinetics. In this paper, we have used theory and experiment to investigate the effects of the buffer-gas parameters on the densities of the elemental constituents in plasma, i.e. the Cu, Br, and H/H_2 species. The theory is tested directly against "Hook" method measurements of the Cu density, and indirectly by examining the effects of buffer-gas conditions on plasma relaxation and voltage-current waveforms. The results, which show that the HBr mass flow rate and the HBr partial pressure separately influence the free Cu density and the volume kinetic reactions that dominate inter-pulse plasma relaxation, have important implications for optimizing laser performance.

II. Theory

The ambient density (i.e. the density averaged in time and throughout the discharge volume) of the reactive elemental species in the discharge are derived by equating their net rate for production in the discharge zone with their transport loss rates out of the discharge. For simplicity, the number of molecular species containing Cu and Br is assumed to be negligible. Though it has been suggested that HBr, Br_2, Cu_nBr_n ($n = 1, 2, 3 \ldots$), and CuH are important discharge reactants (see, e.g., [14] and [20]), their dissociation yield is assumed sufficiently high that their average densities in the plasma are small compared to the atomic Cu and Br populations. In the case of HBr, the number of "intact" molecules in the tube necessary to account for charge recombination of the timescale

of the inter-pulse period, is only a small fraction (∼10%) of the Cu (and Br) densities [15], [16]. Absorption measurements in a 60-mm bore device show that the CuBr monomer density adjacent the tube wall is 3.5×10^{19} m^{-3} [17] (or $< 3\%$ of the typical free Cu atom density), and is $< 0.5 \times 10^{19}$ m^{-3} (or $< 0.5\%$ of the free Cu density) in the central region of the tube.

Given that most HBr molecules added to the tube dissociate, the production of H (present in either atomic or dimer form) in the discharge is equal to the mass flow rate of HBr into the tube ($\phi_{\rm HBr}$), whereas the principal loss mechanism is via the tube vent to the vacuum pump. The loss rate can be expressed as the product of the total gas flow rate ($\phi_{\rm tot}$) and their concentrations X_H and X_{H2} in the plasma so that under steady-state conditions

$$\phi_{\rm HBr} = (X_H + 2X_{H2}) \cdot \phi_{\rm tot}. \tag{1}$$

In terms of partial pressure (e.g., $p_H = X_H \cdot p_{\rm tot}$ where $p_{\rm tot}$ is the total tube pressure), the expression becomes

$$p_{\rm tot} \cdot \frac{\phi_{\rm HBr}}{\phi_{\rm tot}} = p_H + 2p_{H2}$$

or

$$P_{\rm HBr} = p_{H/H2} \tag{2}$$

where $P_{\rm HBr}$ is the partial pressure of HBr in the incoming gas flow to the laser tube[1], and the partial pressure sum $p_H + 2p_{H2}$, which reflects the number of H atoms in the plasma present as dimers or atoms, hereafter denoted by $p_{H/H2}$.

For Br, the production rate likewise equals $\phi_{\rm HBr}$ which in terms of the number of atoms is given by

$$\frac{dN_{\rm Br}^{+}}{dt} = \frac{\phi_{\rm HBr}}{kT_0}. \tag{3}$$

The Br loss rate from the hot-zone, however, is instead dominated by diffusion as discovered in [13]. This study found that, as soon as gas flow is stopped during otherwise normal operation, the Cu density and CuBr density (and laser output) rapidly decrease in synchrony falling to a small fraction of their initial values within one minute. The rate of loss of Cu from the plasma closely matched the calculated rate for the diffusion loss of Br driven to the electrodes by the partial pressure gradient established by the condensation of Br (as CuBr solid or liquid) in the cooled end zones. For nominal buffer-gas flow rates, the rate of diffusion velocity is faster than the rate of gas flow as discussed in more detail in Section III-B. This loss rate for diffusion is given by [13]

$$\frac{dN_{\rm Br}^{-}}{dt} = \frac{N_{\rm Br}}{\tau_D} \tag{4}$$

where τ_D is the diffusion time constant and $N_{\rm Br}$ is the number of Br atoms in the hot discharge zone. Using a simple treatment of diffusion which assumes the spatial dependence of the density is described by the fundamental mode $\tau_D = l^2/D_{\rm Br}\pi^2$, where $D_{\rm Br}$ is the diffusion coefficient of Br in Ne. Then during steady-state operation, i.e., when

$$\frac{dN_{\rm Br}^{+}}{dt} = \frac{dN_{\rm Br}^{-}}{dt} \tag{5}$$

the average Br density in the hot-zone $\tilde{n}_{\rm Br}$ is

$$\tilde{n}_{\rm Br} = \frac{\tau_D}{kT_oV}\phi_{\rm HBr} \tag{6}$$

where the hot-zone has volume V. An important consequence of this relation is that the Br density is markedly lower ($\sim 1 \times 10^{21}$ m^{-3}, i.e., approximately the same as the Cu density—see below) than previous estimates [18] which assume that the density is proportional to $P_{\rm HBr}$ (i.e., 1×10^{22} m^{-3}).

The free Cu is produced by the discharge dissociation of CuBr molecular byproducts of the Cu metal surface reaction with Br species. Though several possible reactions must be considered in the process [12], the Cu density is more directly estimated using the known chemistry of the Cu halides. Thermodynamic studies of Cu-halides suggests that the major products of the surface reaction are monomers and polymers in which the stoichiometric ratio is 1:1 (e.g., Cu_nBr_n $[n = 1,2,3\ldots]$) [19]. These products immediately vaporise since the temperature of the Cu metal during normal operation (450 °C–850 °C) [20] is greater than dew point for CuBr. A high yield for the forward reaction is expected given the high reactivity of the halogen at the elevated temperatures. In fact, the observed insensitivity of laser output to the surface area of the Cu metal placed in the discharge tube [11], [12], and the low amount of Br compounds observed in the mass spectrum of the tube exhaust gas [15] suggest that the yield approaches unity. If the products are largely dissociated by the discharge as assumed here, free Cu atoms are generated in near 1:1 ratio with the number of HBr molecules entering the tube with the gas flow. Comparison of the published diffusion coefficients shows that diffusion rate of Cu to the end-regions occurs at an almost identical rate to Br ($D_{\rm Br} = 2.5 \times 10^{-5}$ m^{2}s^{-1} [21] and $D_{\rm Cu} = 2.9 \times 10^{-5}$ m^{2}s^{-1} [22] at STP). Therefore, the rates for production and loss for Cu are thus very similar to Br so that

$$\tilde{n}_{\rm Cu} \cong \tilde{n}_{\rm Br}. \tag{7}$$

III. Results and Discussion

A. Experimental

Measurements were performed on a nominally 20-W Cu HyBrID laser with bore diameter of 25 mm and active tube length of 720 mm (active volume 345 cm^3), the details of which have been described previously [13]. The laser was operated with fixed input power (1.2 kW) using a 1-nF storage capacitor charged to 12.5 kV and switched into a 0.5-nF peaking capacitor across the laser tube at the pulse rate 17 kHz.

The Ne–HBr gas mixture was admitted to the anode end of the laser tube via metering valves (Nupro SS-4MBG), and the tube vented from the other via a regulating shut valve to a rotary backing pump. The $\phi_{\rm Ne}$ and $\phi_{\rm HBr}$ values were determined for each meter valve setting by first allowing the discharge tube to

[1]Note that a capitalized symbol is used to differentiate the partial pressure in the incoming gas flow from the partial pressure in the plasma.

cool to approximately room temperature, closing the valve between the backing pump and the discharge tube, and then measuring the rate of rise of pressure. The mass flow rate (sccm) was then given by the product of the rate of pressure rise (in atmospheres per minute) by the enclosed volume (1130 cm^3).

Hook method measurements of the ground-state Cu ($^2S_{1/2}$) density were obtained using the probe beam, interferometer, and interferogram capture apparatus described in [13]. Tube current (I) and voltage (V) waveforms were recorded with a 100-MHz bandwidth digital storage oscilloscope (Tektronix TDS320) using a high voltage probe (Tektronix P6105) and Pearson-type current monitor (Ion Physics Corp. CM10). The waveforms were downloaded to a PC using in-house developed communication software and imported into a spreadsheet for analysis. Values for the time-averaged discharge resistance during the excitation phase were determined by integrating $(V - L \cdot dI/dt)/I\Delta t$ (where the tube inductance $L = 380$ nH was determined using the method described in [23]) over the first half-cycle (Δt) of the damped-sinusoidal of the current pulse. Since the resistance of the discharge is initially very high ($\sim 10^3$ ohms), the resultant average resistance values provide an indication of the plasma resistance in the early portion of the current pulse before the rapid ionization and the collapse of the resistance to low values (< 50 ohms). Though these values are expected to include some systematic error due to the small changes in the plasma inductance during the current pulse [24] and the inherent distortion often introduced when measuring high slew rate voltage pulses, the relative values provide a qualitative indicator of plasma resistance as functions of the buffer-gas conditions.

B. Cu Density

The ambient density of Cu atoms in the plasma is determined from measurements of the ground-state Cu density at the end of the inter-pulse period, at which time the recombination and de-excitation of Cu ions and excited states to the ground state is largely complete (i.e., $< 1\%$ of their peak values [24]). The axial Cu density ($n_{\rm Cu}$) increases monotonically with $\phi_{\rm HBr}$ as shown in Fig. 1(a). Based on radially resolved measurements, the Cu density increases for positions away from the tube axis (except very close to the tube wall where the density diminishes) so that the spatial average ($\tilde{n}_{\rm Cu}$) is typically 40% higher than the density on axis. Using (6), $\tilde{n}_{\rm Br} = 2.8 \times 10^{21} \times \phi_{\rm HBr}(\rm m^{-3})$ for the conditions of Fig. 1 (i.e., $\tau_D = 2.5$ s) where $\phi_{\rm HBr}$ is expressed in units of sccm. A comparison of $\tilde{n}_{\rm Cu}$ with $\tilde{n}_{\rm Br}$ is shown in Fig. 2. For $\phi_{\rm HBr} < 0.5$ sccm, the measured $\tilde{n}_{\rm Cu}$ value is in very good agreement with that predicted by the theory. For higher $\phi_{\rm HBr}$ values (i.e., $\phi_{\rm HBr} > 0.5$ sccm), there is an increasing shortfall in $\tilde{n}_{\rm Cu}$ below the theoretical values. We interpret this shortfall as evidence for the invalidity of the assumption that the dissociation yield is near unity when the levels of halogen reactant added to the plasma are very high. Since CuBr dissociation is endothermic (3.5 eV is required to dissociate the monomer [19]), the density of free Cu must ultimately saturate with increasing $\phi_{\rm HBr}$ and an increasing fraction of Br atoms are expected to be present in CuBr (monomers and polymers). This saturation is also exacerbated for the higher $\phi_{\rm HBr}$ values due to a decrease in

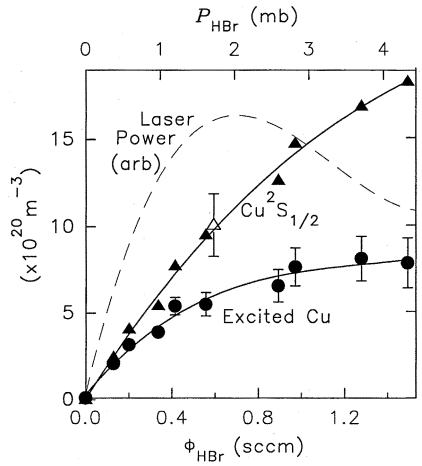

Fig. 1. (a) Prepulse $Cu^2S_{1/2}$ density (solid triangles) and the laser output (broken line) as a function $\phi_{\rm HBr}$. Also shown is the number density of Cu atoms excited during the excitation phase (solid circles), i.e., the overall decrease in the ground-state density that occurs during the excitation pulse. Operating conditions: $p_{\rm tot} = 42$ mbar and $\phi_{\rm Ne} = 14.5$ sccm. The hollow triangle with the associated error bar indicates the range of pre-pulse $Cu^2S_{1/2}$ densities obtained for $\phi_{\rm Ne} < 40$ sccm obtained for the operating conditions corresponding to Fig. 3.

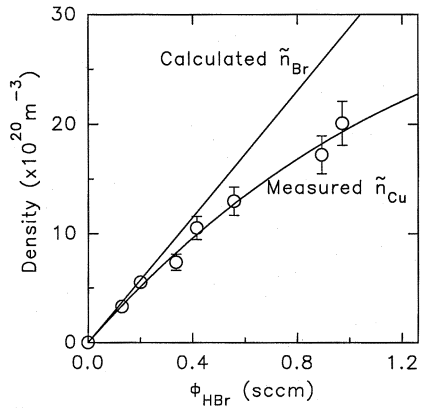

Fig. 2. Comparison of the Br and $Cu^2S_{1/2}$ densities (spatially averaged) as a function of $\phi_{\rm HBr}$. The Br density $\tilde{n}_{\rm Br}$ is calculated assuming diffusion loss from the discharge, driven by the density gradient to the cooled electrodes where the Br density is zero.

electrical energy coupled into the plasma (as discussed in Section III-C3).

This theory predicts no explicit dependence of the Cu density on $P_{\rm HBr}$ in good agreement with that observed when varying the Ne mass flow rate ($\phi_{\rm Ne}$) in the range < 40 sccm with $\phi_{\rm HBr}$ constant. As shown in Fig. 3, the pre-pulse Cu density on-axis remains essentially constant in the range of values denoted by the hollow triangle and associated error bar in Fig. 1 while $P_{\rm HBr}$ increases threefold (i.e., from 1 to 3 mbar). The theory's validity does not extend to gas flow rates > 40 sccm, however, due to the increasing effects of convective gas transport by the buffer-gas flow. The average flow velocity v of the gas in the hot zone is obtained from the flow rate using

$$v = \frac{\phi}{PA} \cdot \frac{\tilde{T}_g}{T_o} \tag{8}$$

where A is the tube cross-sectional area and $\tilde{T}_g$ is the spatial averaged gas temperature. For operating conditions corresponding

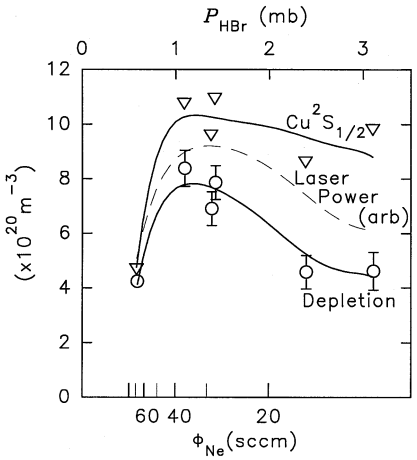

Fig. 3. Prepulse $Cu^2S_{1/2}$ density on axis, the Cu density excited during the excitation phase (depletion) and the laser output power (dashed curve) as functions of $P_{\rm HBr}$ for constant $\phi_{\rm HBr}$. Operating conditions: $\phi_{\rm HBr} = 0.6$ sccm, $p_{\rm tot} = 67$ mbar.

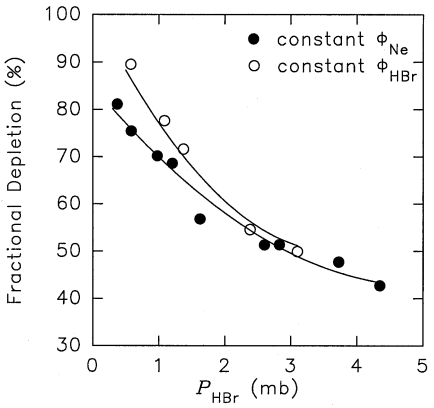

Fig. 4. The fraction of $Cu^2S_{1/2}$ atoms excited during the discharge pulse as a function of $P_{\rm HBr}$ for fixed $\phi_{\rm Ne}$ (filled symbols) and fixed $\phi_{\rm HBr}$ (hollow symbols).

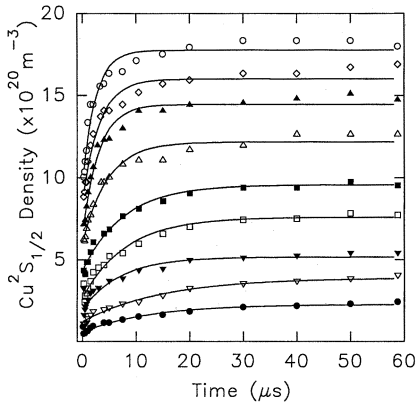

Fig. 5. On-axis population histories of the $Cu^2S_{1/2}$ state for $\phi_{\rm HBr} = 0.1$-1.5 sccm with single-exponential (3-parameter) curve fits. Time $= 0$ corresponds to the leading edge of green superfluorescence. Operating conditions: $P_{\rm tot} = 42$ mbar and $\phi_{\rm Ne} = 14.5$ sccm.

to Fig. 3, $\tilde{T}_g \sim 1500$ K (as determined using the formula in [13]) and the flow velocity is equal to the diffusion speed (i.e. $l/\tau_D \sim 18\text{cm} \cdot \text{s}^{-1}$) when $\phi_{\rm Ne} \sim 65$ sccm. The decrease in Cu density observed for $\phi_{\rm Ne} > 40$ sccm is, therefore, deduced to correspond to the increasing effect of convective transport of reactants from the hot zone. Note that, even for the higher flow rates used in this study, convective cooling of the tube surfaces is not significant since the power required to heat the gas to the average gas temperature ($\sim 10\,\text{W/sccm}$) is negligible compared to the total power deposited in discharge tube. Moreover, convective cooling of the plasma is also negligible (contrary to that suggested in [12]) since the diffusion rate of heat through the plasma ($\sim 10^3$ cms^{-1} [25]) is orders of magnitude faster than typical gas flow velocities (< 20 cms^{-1}).

C. Other Plasma Variables

As the methods for measuring the absolute densities of the other key atomic (H, Br) and molecular (Cu_nBr_n, HBr) species in the discharge are not well developed, the effects of $P_{\rm HBr}$ and $\phi_{\rm HBr}$ on the density of these other components of the plasma were investigated by analysing measurements of Cu excitation, inter-pulse recovery rate, and voltage–current waveforms.

1) Cu Excitation During the Discharge Pulse: The number of ground-state Cu atoms excited to higher states by the discharge excitation pulse, which is evaluated from the difference in the ground-state density prior to and immediately after the excitation pulse, is plotted as functions of $P_{\rm HBr}$ and $\phi_{\rm HBr}$ in Figs. 1 and 3. In absolute terms, these values reflect the Cu density present at the time of the discharge pulse. However, when expressed as a fraction of the pre-pulse Cu atom density as shown in Fig. 4, it is revealed that Cu excitation is essentially characterized by $P_{\rm HBr}$; the fraction of Cu excited decreases monotonically from 90% to 40% when increasing $P_{\rm HBr}$ from 0.3 to 4.5 mbar for both fixed or varying $\phi_{\rm HBr}$. $P_{\rm HBr}$ is, therefore, deduced to directly influence the efficiency of inelastic electron–Cu collisions, whereas the dependence on $\phi_{\rm HBr}$ is much weaker.

The dependence of $p_{H/H2}$ on $P_{\rm HBr}$ predicted by the theory is consistent with this observed decrease in Cu excitation efficiency. The increased rate for inelastic collisions with H and H_2 during the excitation phase diverts energy from the excitation of Cu (and ultimately reduces the laser efficiency as noted below). It is this mechanism which is believed to be responsible for the decrease in conventional copper vapor laser efficiency when increasing the added H_2 partial pressure above a few percent [26]. Based on the relatively minor effect of $\phi_{\rm HBr}$ on the Cu excitation efficiency, the rate for inelastic collisions between atomic Br and electrons is much lower.

2) Inter-Pulse Plasma Relaxation: During the inter-pulse period, the Cu density increases monotonically, as shown in Fig. 5 for the conditions of Fig. 1 (i.e., by increasing $\phi_{\rm HBr}$ for fixed $\phi_{\rm Ne}$). Least-squares curve fits to the data points reveal that the density regrowth approximately follows the form of a single-exponential function (i.e. $n_{\rm Cu}(t) \propto 1 - e^{-t/\tau}$). Though there is evidence of a two-stage recovery, particularly for $\phi_{\rm HBr} > 1$ sccm, the recovery rate constant τ^{-1} is a good parameter for characterizing the relative recovery rates. As shown in Fig. 6, the rate constant increases linearly (at the rate $\sim 0.1\ \mu\text{s}^{-1}\text{mbar}^{-1}$) over the investigated range of $P_{\rm HBr}$, with essentially the same linear relationship observed when either

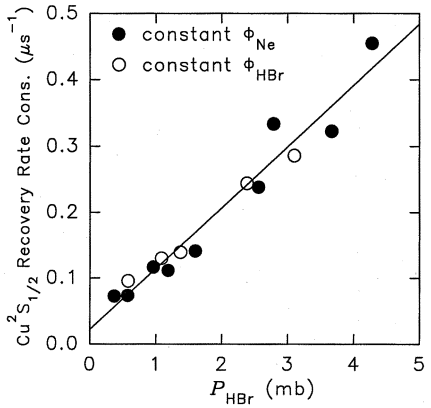

Fig. 6. Rate constant for recovery time constant of the $Cu^2S_{1/2}$ density on-axis during the interpulse period as a function of $P_{\rm HBr}$ for constant $\phi_{\rm Ne}$ (filled symbols) and constant $\phi_{\rm HBr}$ (hollow symbols).

varying $P_{\rm HBr}$ with $\phi_{\rm HBr}$ constant (i.e., by varying $\phi_{\rm Ne}$) or with $\phi_{\rm Ne}$ constant (i.e., by varying $\phi_{\rm HBr}$). The rate of recovery of the Cu ground-state density during the inter-pulse period is thus also strongly characterized by $P_{\rm HBr}$.

According to the theory, then, the plasma species most strongly influencing the rate of inter-pulse plasma relaxation are H and H_2. Though H and H_2 assist via electron cooling [26], the greatly accelerated rate of Cu regrowth observed when also adding halogens to conventional copper vapor lasers [27] unambiguously demonstrates the large accelerating effect of the combined presence of H and halogen species on the rate of plasma relaxation. The dissociative attachment (DA) of electrons to HBr with subsequent mutual neutralization of Br^- with the ionized Cu is presumed to be the major reaction channel which facilitates the accelerated relaxation. Increasing the H_2/H density is thus expected to increase the plasma relaxation rate via the HBr formation reactions

$$H_2 + Br \Leftrightarrow HBr + H \tag{9}$$

$$H + CuBr \Leftrightarrow HBr + Cu \tag{10}$$

$$H + Br^- \Leftrightarrow HBr + e^-. \tag{11}$$

Increasing the Br density would similarly lead to increased numbers of HBr in the plasma. However, no significant increase in the plasma relaxation rate is observed when increasing $\phi_{\rm HBr}$ alone (i.e., for constant $P_{\rm HBr}$). A possible explanation for this is that the dissociative attachment and mutual neutralization reactions do not ultimately limit the rate of ground-state recovery and that other mechanisms involving the H/H_2 density influence the Cu regrowth more directly.

Such a possible direct mechanism is the de-excitation of Cu metastables to the ground-state involving H_2. Since it is energetically favorable for the mutual neutralization process to leave Cu atoms in the excited levels [28] which rapidly relax to the metastable states by radiative decay, the metastable states form a "bottle neck" for the relaxing Cu species. The electron collisional deactivation, which is the main mechanism for de-excitation in conventional copper vapor lasers, is not so prevalent in the Cu HyBrID discharge due to the reduced free electron density. In order to accurately model the measured metastable decay and ground-state recovery in pulse afterglow of kinetically enhanced copper vapor lasers, Carman *et al.* [29] introduced the H_2 reaction sequence

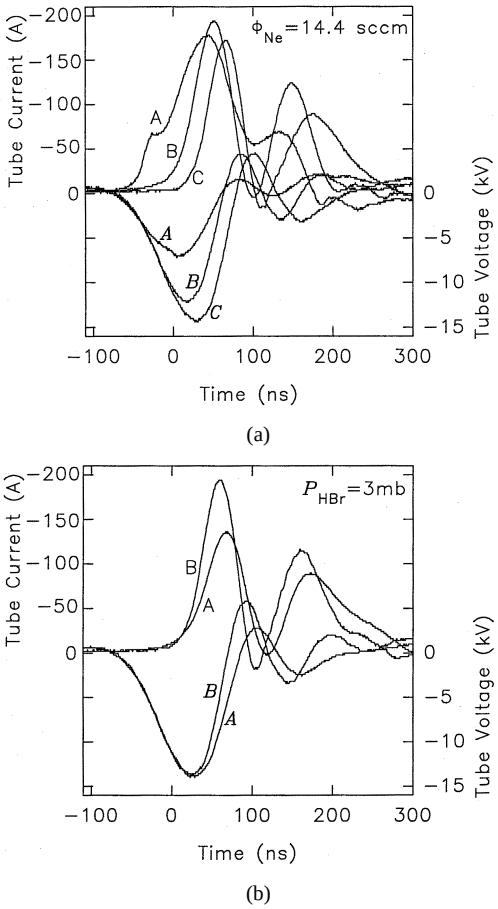

Fig. 7. (a) Voltage (A, B, C) and current (A,B,C – inverted) waveforms for $\phi_{\rm HBr}$ =0.13, 0.59, and 1.5 sccm for constant $\phi_{\rm Ne}$ (14.4 sccm). (b) Voltage (A, B) and current (A,B – inverted) waveforms for $\phi_{\rm HBr} = 0.59$ and 0.96 sccm for constant $P_{\rm HBr}$ (3 mbar).

$$Cu^*(^2D) + H_2(v > 1) \Rightarrow CuH + H \Rightarrow Cu + H_2(v + 3) \tag{12}$$

where energy is transferred from the excited Cu atom to vibrationally excite H_2. For the present device, the increasing Cu regrowth rate with $P_{\rm HBr}$ (and thus $p_{H/H2}$) suggests that this reaction is also important in Cu HyBrID lasers.

3) Current–Voltage Waveforms: The separate effects of $P_{\rm HBr}$ and $\phi_{\rm HBr}$ on the plasma composition are also evident in the tube V-I waveforms. Referring to Fig. 7(a), example waveforms for below (0.4 mbar), near (1.5 mbar), and above (5.2 mbar) optimal $P_{\rm HBr}$ values (for fixed $\phi_{\rm Ne}$) show that the discharge resistance during the early part of the current pulse increases markedly when increasing $P_{\rm HBr}$. For $P_{\rm HBr} < 1$ mbar, the step on the leading edge of the current pulse is characteristic of a high population of remnant electrons at the time voltage is applied to the discharge tube [30]. As $P_{\rm HBr}$ is increased, the amplitude of the current step diminishes and the peak tube voltage is increased. The time-averaged plasma resistance during the early part of the excitation phase increases monotonically with $P_{\rm HBr}$, as shown in Fig. 8(a) (values obtained using the method described in Section II). The resistance also increases in a similar fashion when increasing $P_{\rm HBr}$ with $\phi_{\rm HBr}$

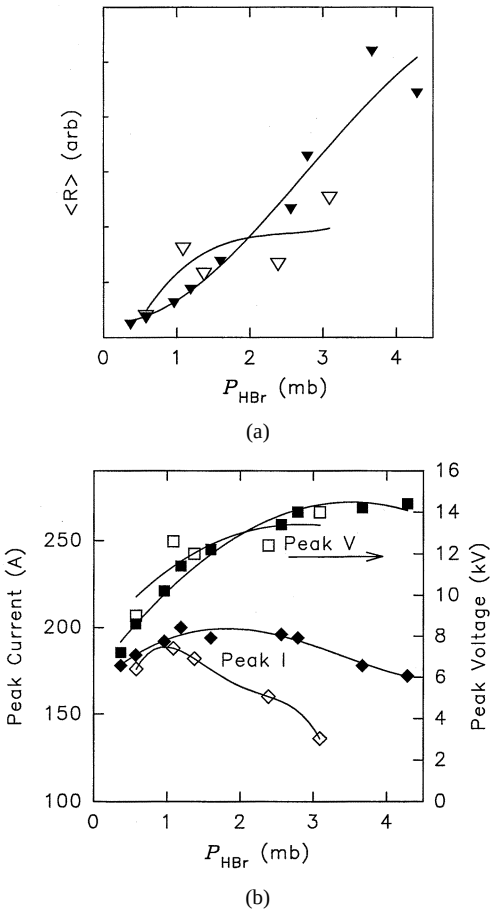

Fig. 8. (a) Time-averaged plasma resistance ($\langle R \rangle$) and (b) the peak value of tube voltage (squares) and current (diamonds) as functions of $P_{\rm HBr}$ for constant $\phi_{\rm Ne}$ (solid symbols) and constant $\phi_{\rm HBr}$ (hollow symbols).

constant [see hollow symbols in Fig. 8(a)]. Thus, $P_{\rm HBr}$ largely characterizes the plasma resistance early in the development of the excitation pulse.

The explicit effects of $\phi_{\rm HBr}$ on the V–I waveforms are most evident later in the excitation phase when the tube current is near maximum. A comparison of the V–I waveforms for constant $P_{\rm HBr}$, as shown in Fig. 7(b), reveals that increasing $\phi_{\rm HBr}$ by 40% brings about an approximately proportional increase in the peak amplitude of the tube current whereas prior to the discharge current increasing to 20% of its peak value the voltage and current waveform are unaffected.

These effects of $P_{\rm HBr}$ and $\phi_{\rm HBr}$ on the V–I waveforms are also in good qualitative agreement with the theory. The increase in the initial plasma resistance for high $P_{\rm HBr}$ presumably reflects the aforementioned action of HBr (via attachment), and to a lesser extent H_2 and H species (via electron cooling), in reducing the free electron density prior to the excitation pulse. However, well after discharge breakdown, the increased rate of current growth with $\phi_{\rm HBr}$ is attributed to the higher density of Cu atoms available for ionization during excitation. Similar increases in current growth and peak current are noted when raising the Cu density in our high-temperature copper vapor lasers (kinetically enhanced and conventional). Since Cu atoms have the lowest ionization potential of the major plasma constituents, they provide the major source of free electrons during the excitation phase. As a result, the evolution of discharge current is sensitive to the Cu density and $\phi_{\rm HBr}$ as observed.

D. Plasma Conditions at Maximum Output Power

1) Comparison With Other Cu Lasers: The dependence of the laser output power on $\phi_{\rm HBr}$ and $P_{\rm HBr}$ is shown by the broken lines in Figs. 1 and 3, respectively. Maximum output power occurs for $\phi_{\rm HBr} \sim 0.7$ sccm and $P_{\rm HBr}$ =1–2 mbar, which correspond to ambient plasma densities $\tilde{n}_{\rm Br} = \tilde{n}_{\rm Cu} = 1.5 \times 10^{21}$ m^{-3} and $p_{H/H2}$ = 1-2 mbar. Interestingly, this plasma composition is very similar to that of other halogen-enhanced systems. As shown in Table I, the Cu, Br, and H/H_2 densities for each of the laser types are within a factor ~ 2, which is remarkable agreement given that the tube dimensions and operating conditions (i.e., pulse rate and tube temperature) vary markedly between each device. Several similarities in the plasma properties of the Cu HyBrID and Ne:H_2:CuBr lasers have also been previously noted in [15]. The plasma composition deduced for the Cu HyBrID laser in this study is the first quantitative evidence that it is the chemical reactions that seed each elemental constituent into the discharge that fundamentally distinguish the Cu HyBrID laser from the other systems, rather than the plasma composition.

Assuming that the densities in Table I are near optimum for maximum output, the HBr mass flow rate and partial pressure can be predicted using (2)–(7) for Cu HyBrID lasers of different size. Table II lists the operating conditions at maximum output power for other Cu HyBrID lasers reported in the literature which have bore diameters in the range of 1.25 –10 cm. Of the 14 listed, only two lasers have $P_{\rm HBr}$ outside the expected range 1–2 mbar. The widespread agreement for the $P_{\rm HBr}$ values presumably reflects the important effect of the H and H_2 densities we observe on the inter-pulse plasma relaxation rate and the Cu excitation efficiency.

The $\phi_{\rm HBr}$ values, on the other hand, differ notably between devices since the diffusion loss rates are a function of tube geometry, gas temperature and gas pressure. Assuming the typical Cu density $\tilde{n}_{\rm Cu} = 2 \times 10^{21}$ m^{-3} for each device, $\phi_{\rm HBr}$ has been calculated using (6) and (7) for each of the tubes and compared to the reported value. The gas temperature, which significantly influences the diffusion rate, was calculated from the average input power density ρ deposited in the plasma (estimated to be half the switched power) using the relation[2]

$$T(r) = \left[T_w^{m+1} - \frac{\rho(m+1)}{\lambda_0 R^2} \left(r^2 R^2 - \frac{r^4}{4} - \frac{3R^4}{4} \right) \right]^{1/(m+1)} \tag{13}$$

where R is the tube radius, and λ_0 and m are constants for the neon thermal conductivity K which varies according to $K = \lambda_0 T^m$ [25]. Good agreement between the theoretical and experimental $\phi_{\rm HBr}$ values (see also Table II) is obtained (i.e., within a factor of 2), particularly for the lasers with bore diameter $\leq$ 25 mm (where the agreement is within 30%). The most notable disagreement is observed for the devices of Ohzu *et al.* [34]–[36] where the values differ by a factor of three to four. Given the often large uncertainties in the measured buffer-gas flow rates and the simplicity of the theory, the agreement serves

[2]Formula is reproduced from [13] in corrected form.

TABLE I
COMPARISON OF THE CU, HALOGEN, AND HYDROGEN DENSITIES FOR THE CU HYBRID LASER, THE KE-CVL AND THE CUBR LASERS WITH H_2 ADDITIVE

	N_{Cu} (axis) ($\times 10^{21} m^{-3}$)	$\tilde{n}_{Cu}$ ($\times 10^{21} m^{-3}$)	$\tilde{n}_{Br}$ ($\times 10^{21} m^{-3}$)	$p_H + 2p_{H2}$ (mb)
Cu HyBrID Laser	1.0	1.5	1.5 (Eq. 7)	1-2 (Eq. 2)
KE-CVL[29]	1.1	1.6	3* ($\tilde{n}_{Cl}$)	0.8
CuBr:H_2 Laser[32]	2.2	-	2.2**	0.8

* Based on model predictions. ** Assuming the Cu and Br densities are in the ratio 1:1.

TABLE II
A COMPARISON OF THE HBR MASS FLOW RATE ϕ_{HBr} FOR CU HYBRID LASERS REPORTED IN THE LITERATURE AT CONDITIONS MAXIMUM OUTPUT POWER WITH THEORETICAL PREDICTIONS FOR ϕ_{HBr} DETERMINED FROM THE OPERATING CONDITIONS AT MAXIMUM OUTPUT POWER. THE THEORETICAL VALUE ASSUMES AN AVERAGE CU DENSITY $\bar{n}_{Cu} = 2 \times 10^{21}$ m^{-3}

Tube diameter	Tube length	Input power	ϕ_{tot}	P_{tot}	P_{HBr}	ϕ_{HBr} *measured*	*theory*	
cm	cm	kW	sccm	mb	mb	sccm	sccm	Reference
1.25	30	1.4	13.3	50	3.9	1.04	0.72	Little et al [12]
1.3	30	0.8	8.3-16.7	70	1.6	0.18-0.37	0.34	Livingstone et al[34]
2.2	72	1.2	14.3	55	1.3	0.34	0.36	Mildren et al[11]
2.5	72	1.2	14.5	42	2.0	0.69	0.59	This Study
2.5	70	1.8	30	40-100	2.0	0.6-1.5	0.4-0.9	Riva et al[35]
4	120	4.6	66.7	38	2.0	3.50	2.07	Ohzu et al[36]
4.5	120	3.5	8.3-16.7	22	1.6	0.59-1.18	3.42	Jones et al[10]
6	120	6.4	66.7	38	2.0	3.50	6.24	Ohzu et al[36]
6	200	5.4	33.3-66.7	35	5.0	4.76-9.52	2.19	Jones et al[31]
6	200	3.7	50.0-66.7	32	1.6-2.2	3.33-3.54	1.78	Jones et al[5]
8	120	6.4	66.7	38	2.4	4.21	11.1	Ohzu et al[36]
8	120	5.8	83.3	26	1.4	4.50	14.5	Ohzu et al[37]
8	120	5.1	66.7	29	1.4	3.17	11.9	Ohzu et al[38]
10	300	8.0	16.7-83.3	35	1.7	0.80-4.00	4.03	Le Guyadec et al[8]

to validate the theory for a wide range of operating conditions and tube sizes.

2) Buffer-Gas Optimization: When raising the laser output power from turn-on at room-temperature, often the most practically convenient method employed for optimizing the gas mixture uses a fixed buffer-gas flow rate through the tube while the HBr partial pressure is optimized for maximum output power. It is thus necessary to adjust the flow rate each time iteratively re-optimizing P_{HBr} in order to optimize both ϕ_{HBr} and P_{HBr}. This study, however, suggests that optimization is achieved more directly by setting P_{HBr} to 1–2 mbar so that only the flow rate is adjusted to gain maximum output. For this, it is necessary to increase ϕ_{HBr} and ϕ_{Ne} in proportion, which can be conveniently achieved in practice, for example, by using a premixture of HBr and Ne in the concentration corresponding to the desired HBr partial pressure (e.g., 2%–4% HBr in Ne for $p_{tot} = 50$ mbar) and by introducing the mixture into the tube using a single flow control valve. Maximum output power is then generally observed when the peak tube current is maximum (refer to Fig. 8).

This capability to vary the Cu density in the plasma in this manner without significantly affecting the species which control plasma relaxation may realize further gains in output power and efficiency. For the present device, for example, laser performance was only investigated for $P_{HBr} = 1$–2 mbar and for $\tilde{n}_{Cu} < 1.5 \times 10^{21}$ m^{-3}. In the light of this study, more laser output from the present device would have been likely by using higher ϕ_{HBr} values that correspond to Cu densities $> 1.0 \times 10^{21}$ m^{-3} while keeping P_{HBr} constant at ~ 1.5 mbar. Note that the Cu density is limited at high flow rates by convective removal of the Br reactant so that the Cu density only increases with flow rate for values for which diffusion dominates over convective transport. Since such conditions prevail for gas flow rates < 50 sccm (refer Section III-B), it is predicted that Cu densities up to 2-3 $\times 10^{21}$ m^{-3} (corresponding to $\phi_{HBr} \sim 2$ sccm) are achievable in the present device. When increasing Cu density, the optimal energy of excitation pulses will increase due to the additional discharge energy needed to dissociate the molecular precursors and then to excite the free Cu to the upper laser levels. Higher excitation voltages are therefore favored when scaling output with Cu density. Note that the situation analogous to thermal runaway in high-temperature Cu vapor lasers, in which the energy coupling into the tube and Cu density increase through positive feedback, is absent in Cu HyBrID lasers since the Cu density and tube temperature are not coupled in the same manner. As a result, high-efficiency output is more easily obtained over a much larger range compared to non-HyBrID lasers in which the Cu vapor density is strongly coupled to the input power and tube insulation.

The results also suggest directions for the optimization of laser dimensions. Tube geometries which minimize the rate of Br diffusion loss will enable higher Cu densities to be achieved for a given total gas flow rate and P_{HBr}. Since the diffusion loss rate is proportional to l^{-2} [refer to (4)], longer tubes will enable access to the advantages that may be gained by operating with elevated Cu densities, such as increased efficiency and specific output power.

IV. Conclusions

Theoretical and experimental investigations show that the ambient densities of Cu and hydrogen in the discharge are influenced separately by the buffer-gas parameters ϕ_{HBr} and P_{HBr}. The theory, which predicts well the optimal buffer-gas conditions for Cu HyBrID lasers reported to date in the literature, provides an important basis for more comprehensive modeling studies of the laser discharge. The results suggest that optimized buffer-gas conditions are obtained more directly by first fixing P_{HBr} in the range 1–2 mbar and then adjusting the mass flow rate for maximum output power.

Acknowledgment

The author thanks Dr. R. Carman for helpful discussions and comments, and Mr. D. Baer and Mr. J. Tocher for their technical assistance.

References

[1] C. E. Little, D. R. Jones, S. A. Fairlie, and C. G. Whyte, "Metal HyBrID lasers," in *Pulsed Metal Vapor Lasers*, C. E. Little and N. V. Sabotinov, Eds. Dordrecht, The Netherlands: Kluwer, 1996, pp. 125–136.

[2] M. J. Withford, D. J. W. Brown, R. J. Carman, and J. A. Piper, "Kinetically enhanced copper vapor lasers employing H_2-HCL-Ne buffer gas mixtures," *Opt. Commun.*, vol. 154, pp. 160–166, 1998.

[3] D. N. Astadjov, N. V. Sabotinov, and N. K. Vuchkov, "Effect of hydrogen additive on CuBr laser power and efficiency," *Opt. Commun.*, vol. 56, pp. 279–282, 1985.

[4] D. N. Astadjov, N. K. Vuchkov, and N. V. Sabotinov, "Parametric study of the CuBr laser with hydrogen additives," *IEEE J. Quantum Electron.*, vol. 24, pp. 1927–1935, Sept. 1988.

[5] D. R. Jones, A. Maitland, and C. E. Little, "A high efficiency 200 W average power copper HybrID laser," *IEEE J. Quantum Electron.*, vol. 30, pp. 2385–2390, Oct. 1994.

[6] N. V. Sabotinov, F. Akerboom, D. R. Jones, A. Maitland, and C. E. Little, "A copper HybrID laser with 2 $\mathrm{W/cm^3}$ specific output power," *IEEE J. Quantum Electron.*, vol. 31, pp. 747–753, Apr. 1995.

[7] R. P. Mildren, D. R. Jones, and D. J. W. Brown, "A 100 W, near diffraction limited, copper HybrID laser oscillator," *J. Phys. D: Appl. Phys.*, vol. 31, pp. 1812–1816, 1998.

[8] E. Le Guyadec, P. Coutance, G. Bertrand, and C. Peltier, "A 280-W average power Cu-Ne-HBR laser amplifier," *IEEE J. Quantum Electron.*, vol. 15, pp. 1616–1622, Nov. 1999.

[9] D. R. Jones, A. Maitland, and C. E. Little, "Radial and temporal laser pulse profiles in a 0.2 kW average power copper HybrID laser," in *Proc. SPIE*, vol. 2118, 1994, pp. 42–50.

[10] D. R. Jones, N. V. Sabotinov, A. Maitland, and C. E. Little, "A high-power high-efficiency Cu-Ne-HBr ($\lambda = 510.6$, 578.2 nm) laser," *Opt. Commun.*, vol. 94, pp. 289–299, 1992.

[11] R. P. Mildren, K. E. Osgood, and J. A. Piper, "Characteristics of copper HybrID-type lasers which use HCl reactive gas," *Opt. Quantum Electron.*, vol. 29, pp. 991–998, 1997.

[12] L. Little and C. E. Little, "Dynamics of the metal seeding process in copper hybrid lasers," in *Proc. SPIE*, vol. 3092, 1998, pp. 285–288.

[13] R. P. Mildren, "The role of buffer-gas flow in Cu HybrID lasers," *IEEE J. Quantum Electron.*, vol. 36, pp. 1145–1150, Oct. 2000.

[14] F. Girard, E. Le Guyadec, and P. Delaporte, "CuH and CuBr absorption measurements and consequences on copper seeding in Cu-HBr laser medium," *J. Appl. Phys.*, vol. 89, pp. 843–848, 2001.

[15] A. A. Isaev, D. R. Jones, C. E. Little, G. G. Petrash, C. G. Whyte, and K. I. Zemskov, "Characteristics of pulsed discharge in copper bromide and copper HybrID lasers," *IEEE J. Quantum Electron.*, vol. 33, pp. 919–926, June 1997.

[16] R. J. Carman, M. J. Withford, D. J. W. Brown, and J. A. Piper, "Influence of the pre-pulse plasma electron density on the performance of elemental copper vapor lasers," *Opt. Commun.*, vol. 157, pp. 99–104, 1998.

[17] P. Coutance and J. P. Pique, "Radial and time-resolved measurement of cuprous bromide concentration in a Cu-HBr laser," *IEEE. J. Quantum Electron.*, vol. 34, pp. 1340–1348, Aug. 1998.

[18] C. E. Little, *Metal Vapor Lasers*. Chichester, U.K.: Wiley, 1999, pp. 161–162.

[19] L. Brewer and N. L. Lofgren, "The thermodynamics of gaseous cuprous chloride, monomer and trimer," *J. Amer. Chem. Soc.*, vol. 72, pp. 3038–3045, 1950.

[20] C. E. Little, D. R. Jones, S. A. Fairlie, and C. G. Whyte, "Metal HybrID lasers," in *Pulsed Metal Vapor Lasers*, C. E. Little and N. V. Sabotinov, Eds. Dordrecht, The Netherlands: Kluwer, 1996, pp. 125–146.

[21] M.-D. Hwang, R.-C. Jiang, and T.-M. Su, "Measurements of the diffusion coefficients of atomic bromine in rate gases," *J. Chem. Phys.*, vol. 91, pp. 1626–1630, 1989.

[22] Y. S. Cho, D. W. Ernie, and H. J. Oskam, "Energy transfer processes in decaying neon-copper gaseous plasmas," *Phys. Rev. A*, vol. 30, pp. 1760–1765, 1984.

[23] J. L. Pack and I. Liberman, "Voltage and current measurements for fast pulsed high current discharges," *Rev. Sci. Instrum.*, vol. 52, pp. 1580–1582, 1981.

[24] C. G. Whyte, "The Kinetics of Copper HyBrID Lasers," PhD , Univ. of St. Andrews, St. Andrews, Scotland, U.K., 1995.

[25] J. Kestin, E. Knierim, E. A. Mason, B. Najafi, S. T. Ro, and M. Waldman, "Equilibrium and transport properties of the noble gases and their mixtures at low density," *J. Phys. Chem. Ref. Data*, vol. 13, pp. 229–305, 1984.

[26] M. J. Withford, D. J. W. Brown, and J. A. Piper, "Investigation of the effects of hydrogen and deuterium on copper vapor laser performance," *Opt. Commun.*, vol. 110, pp. 699–707, 1994.

[27] R. P. Mildren, M. J. Withford, D. J. W. Brown, R. J. Carman, and J. A. Piper, "Afterglow ground-state copper density behavior in kinetically-enhanced copper vapor lasers," *IEEE J. Quantum Electron.*, vol. 34, pp. 2275–2278, Dec. 1998.

[28] R. J. Carman, R. P. Mildren, M. J. Withford, D. J. W. Brown, and J. A. Piper, "Modeling the plasma kinetics in a kinetically enhanced copper vapor laser utilizing $\mathrm{HCl} + \mathrm{H_2}$ admixtures," *IEEE J. Quantum Electron.*, vol. 36, pp. 438–449, Apr. 2000.

[29] R. J. Carman, R. P. Mildren, J. A. Piper, G. D. Marshall, and D. W. Coutts, "Plasma kinetics issues for repetition rate scaling of kinetically enhanced copper vapor lasers," in *Proc. SPIE*, vol. 4184, 2001, pp. 215–218.

[30] D. R. Jones, S. N. Halliwell, and C. E. Little, "Influence of remanent electron density on the performance of copper HybrID lasers," *Opt. Commun.*, vol. 111, pp. 394–402, 1994.

[31] D. N. Astadjov, A. A. Isaev, G. G. Petrash, I. V. Ponomarev, N. V. Sabotinov, and N. K. Vuchkov, "Temporal and radial evolution of the populations of CuI levels in the CuBr vapor laser," *IEEE J. Quantum Electron.*, vol. 28, pp. 1966–1969, Oct. 1992.

[32] E. S. Livingstone, D. R. Jones, A. Maitland, and C. E. Little, "Characteristics of a copper bromide laser with flowing Ne-HBr buffer gas," *Opt. Quantum Electron.*, vol. 24, pp. 73–82, 1992.

[33] R. Riva, J. T. Watanabe, C. L. dos Santos, N. A. S. Rodrigues, and C. Schwab, "Maintaining efficiency of a Cu-HybrID laser while changing laser parameter," in *Proc. SPIE*, vol. 4184, 2001, pp. 219–223.

[34] A. Ohzu, M. Kato, and Y. Maruyama, "Scaling dependence of a low temperature operated copper vapor laser," *Jpn. J. Appl. Phys.*, vol. 39, pp. 5118–5123, 2000.

[35] ——, "Growth of dendrites in a large bore HyBrID copper vapor laser," *Opt. Laser Tech.*, vol. 32, pp. 101–105, 2000.

[36] ——, "Comparative study of gas composition in a low temperature operated copper vapor laser," *Opt. Commun.*, vol. 177, pp. 355–361, 2000.

Richard P. Mildren was born in Elizabeth, South Australia, in 1968. He received the B.Sc. (Hons.) degree in physics from the University of Adelaide, Adelaide, Australia, in 1989 and the Ph.D. from the Centre for Laser and Applications, Macquarie University, Sydney, Australia, for experimental studies of barium vapor laser kinetics using the interferometric "Hook" technique.

In 1995, he was a awarded a postdoctoral scholarship at the Italian National Research Council, Pisa, Italy, to study spectroscopical analysis techniques for laser produced plasmas. In 1996, he rejoined the Centre for Lasers and Applications and obtained an Australian Postdoctoral Fellowship to investigate the kinetics of halogen-enhanced copper laser systems. His research interests include high-power lasers, laser spectroscopy of metal vapor discharges, and VUV generation from gas discharges.